First publ. in: Journal of Applied Physics 101 (2007), 103912

Intrinsic ferromagnetism versus phase segregation in Mn-doped Ge

E. Biegger,[a] L. Stäheli, M. Fonin, and U. Rüdiger
Fachbereich Physik, Universität Konstanz, 78457 Konstanz, Germany

Yu. S. Dedkov
Institut für Festkörperphysik, Technische Universität Dresden, 01062 Dresden, Germany

We report on a detailed study of structural, magnetic, and electronic properties of Mn_xGe_{1-x} single crystals $(0<x<0.1)$ prepared by the Bridgman's crystal growth technique. The chemical distribution of Mn in a Ge matrix investigated by means of energy dispersive x-ray spectroscopy indicates a strong phase separation in the Ge/Mn system. Temperature-dependent magnetization $[M(T)]$ measurements performed on the Mn-poor part containing 1%–3% of Mn reveal magnetic properties similar to those of a $Mn_{11}Ge_8$ reference sample as well as to those of the highly inhomogeneous Mn-rich parts of the sample. X-ray absorption spectroscopy (XAS) at the Mn $L_{2,3}$ absorption edge shows that Mn ions in Mn-rich and Mn-poor parts are in the divalent high-spin state. Resonant valence-band photoelectron spectroscopy (ResPES) was performed at the Mn $2p_{3/2}$ absorption edge for the Mn-poor part. The obtained Mn $3d$ PDOS shows a feature centered at 4.8 eV which is characteristic for the Mn_5Ge_3 phase. We identify the formation of ferromagnetic intermetallic compounds as the most possible origin of ferromagnetism in both Mn-rich and Mn-poor regions of the Mn_xGe_{1-x} samples.

I. INTRODUCTION

Diluted magnetic semiconductors (DMS) have become the subject of intensive research due to the possibility to utilize both charge and spin degrees of freedom in the same material which permits the design of a new generation of spintronic devices with enhanced functionalities. Recently, interest in DMS has been reinspired by the discovery of spontaneous ferromagnetism in Mn-doped GaAs with a Curie temperature (T_C) of about 110 K.[1] Ferromagnetic ordering in the $Ga_{1-x}Mn_xAs$ system can be understood on the basis of mean-field calculations of the Zener's model,[2] which also predicts high T_C ferromagnetism in several Mn-doped semiconducting materials. Recent experimental investigations revealed the presence of ferromagnetic order in Mn-doped Ge thin films[3,4] and in bulk single crystals[5] showing T_C of about 116 and 250 K, respectively. Ferromagnetic order was also reported for epitaxial films of Ge codoped with Mn and Co with T_C of about 270 K.[6] Although much effort has been focused on the investigation of Mn_xGe_{1-x}DMS, the precise origin of the ferromagnetic order in this system is still unclear. In particular, the possibility of phase separation (formation of Mn-rich phases) in the Ge/Mn system and its influence on the magnetic properties of the DMS is the key issue in the field.

In the pioneering work by Cho *et al.*,[5] Mn_xGe_{1-x} DMS single crystals were reported to show ferromagnetic order between 150 and 285 K, as determined from temperature-dependent magnetization measurements. In this early study it was also suggested that Mn incorporates into the Ge host lattice without the formation of intermetallic phases, and the origin of the ferromagnetism in Mn_xGe_{1-x} is therefore intrinsic. Since then, various preparation techniques have been employed in order to produce Mn-doped Ge DMS, including single-crystal growth,[5] molecular beam epitaxy (MBE),[7–9] and ion implantation.[10,11] However, several of the reports on intrinsic ferromagnetism in Mn_xGe_{1-x} DMS have been questioned recently by the structural proofs for the formation of intermetallic ferromagnetic compounds, both in single crystals[12] and low-temperature MBE fabricated films.[8,9] Thus, an identification of phase separation in the Mn-doped Ge system would be helpful for the interpretation of the magnetic properties of Mn_xGe_{1-x}.

In this article we report on the investigation of structural, magnetic, and electronic properties of Mn_xGe_{1-x} samples grown by the Bridgman's crystal growth technique. The chemical distribution of Mn in the Ge matrix investigated by means of energy dispersive x-ray spectroscopy (EDX) clearly shows a strong phase separation between Mn-rich and single-crystalline Mn-poor regions. Temperature-dependent magnetization $[M(T)]$ measurements on Mn-poor parts of the Mn_xGe_{1-x} samples show ferromagnetic behavior between 150 and 285 K, which was compared to that of a reference $Mn_{11}Ge_8$ sample. The electronic properties of the Mn-rich and -poor regions of the Mn_xGe_{1-x} sample were investigated by x-ray absorption spectroscopy (XAS) at Mn $L_{2,3}$ absorption edge as well as valence-band photoemission spectroscopy. Resonant photoelectron spectroscopy (ResPES) was performed at the Mn $2p-3d$ excitation threshold to obtain the partial density of states (PDOS) of Mn $3d$ states in the Mn-poor region.

[a]Electronic mail: erwin.biegger@uni-konstanz.de

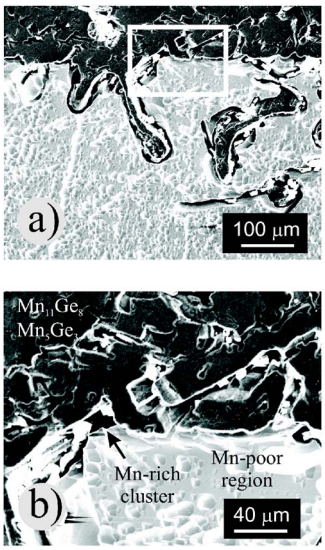

FIG. 1. (a) $640\times460\ \mu m^2$ SEM image of the $Mn_{0.1}Ge_{0.9}$ crystal surface with dark regions corresponding to the Mn-rich phase and bright regions corresponding to the Mn-poor phase. (b) $260\times180\ \mu m^2$ zoom into the field marked in (a). The chemical composition determined by EDX is marked in image (b).

II. EXPERIMENT

Mn_xGe_{1-x} single crystals were prepared by means of the Bridgman's crystal growth technique from high-purity Mn (3*N*) and Ge (5*N*) powders. The overall sample preparation procedure used in this study was close to that of Cho *et al.*[5] In brief, Ge and Mn powders were mixed and encapsulated in a quartz ampoule. The ampoule was heated to 1000 °C in a vertical furnace followed by a 48 h soak. The crystal growth was performed by decreasing the temperature at 0.5 °C/h below the melting point of Ge (937 °C) to about 850 °C and thereafter at 100 °C/h. After the growth the single crystals were cut with a wire saw in order to isolate the distinct parts of the sample. XAS and ResPES experiments were carried out at the RGBL-PGM beam line of BESSY (Berlin). ResPES spectra were collected in the angle-integrated mode with a total energy resolution of 150 meV. The photoemission spectra were normalized to the incident photon flux, which was monitored by detecting the photocurrent from the last gold-covered mirror of the beam line. XAS spectra were obtained by employing the total electron yield method at the Mn $L_{2,3}$ absorption edge with the photon-energy resolution set to 80 meV. After introducing the sample into the UHV chamber at BESSY its surface was cleaned by moderate Ar^+ ion sputtering.

III. RESULTS AND DISCUSSION

A. Structural properties

EDX on a scanning electron microscope (SEM) was performed to investigate the chemical distribution of Mn in the samples. Figure 1 shows a SEM image ($640\times460\ \mu m^2$) of the $Mn_{0.1}Ge_{0.9}$ crystal surface (a) together with a 260 $\times180\ \mu m^2$ zoom (b) into the field marked in (a). Careful EDX analysis at the surface shows a strong phase separation between Mn-rich and Mn-poor regions. In Mn-poor regions (bright areas in Fig. 1) the Mn content was found to be in the range of 1%–3% or even below the detection limit of EDX, showing no Mn-rich inclusions down to the resolution limit of EDX (about 1 μm). Mn-rich regions (dark areas in Fig. 1) which are smaller than Mn-poor regions show higher Mn concentration, with some regions having the composition close to Mn_5Ge_3 and $Mn_{11}Ge_8$ phases. We found that the Mn content in the Mn-poor phase was similar for all samples with different initial Mn content. In the following, we will distinguish between the single-crystalline homogeneous Mn-poor phase containing 1%–3% of Mn and the highly inhomogeneous Mn-rich phase.

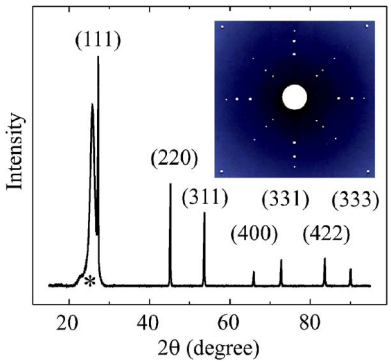

FIG. 2. $\theta-2\theta$ x-ray powder diffraction pattern of a Mn-poor part of the $Mn_{0.08}Ge_{0.92}$ sample. The peak labeled with an asterisk is due to the sample holder. The inset shows a Laue pattern taken along the [100] direction of the single-crystal $Mn_{0.08}Ge_{0.92}$ sample, confirming the good crystalline quality of the Mn-poor region.

The crystal structure of the Mn-poor phase was investigated by $\theta-2\theta$ x-ray powder diffraction (XRD) as well as by Laue back reflection on single crystals. Figure 2 shows an XRD pattern of the Mn-poor region of the $Mn_{0.08}Ge_{0.92}$ sample indicating good crystalline quality of the samples without any impurity phases. The XRD pattern was that expected for the diamond structure of Ge. However, the Mn-rich parts of the single crystals showed additional peaks which can be attributed to Mn_5Ge_3 and $Mn_{11}Ge_8$ phases (not shown). The Laue diffraction pattern measured in the [100] direction of the Mn-poor region of $Mn_{0.08}Ge_{0.92}$ sample is shown as an inset in Fig. 2. A fourfold symmetry was observed due to the [100] direction of the single crystal, confirming the single-crystal quality of the Mn-poor phase.

B. Magnetic properties

Magnetic properties of the samples were studied by means of superconducting quantum interference device (SQUID) magnetometry. For this purpose the single-crystal Mn-poor part was separated from the rest of the crystal. Figure 3(a) shows a typical temperature-dependent magnetization measured in an applied field of 10 mT in zero-field cooled (ZFC) and field-cooled (FC) conditions. In the $M(T)$ curves two distinct transitions can be identified at about 150 and 285 K. Only in the region between 150 and 285 K a hysteresis in the $M(H)$ dependence could be observed [see Fig. 4(a)]. Similar magnetic transitions in Mn_xGe_{1-x} single crystals were observed by Cho *et al.*[5] and attributed to an antiferromagnetic state to ferromagnetic state transition at

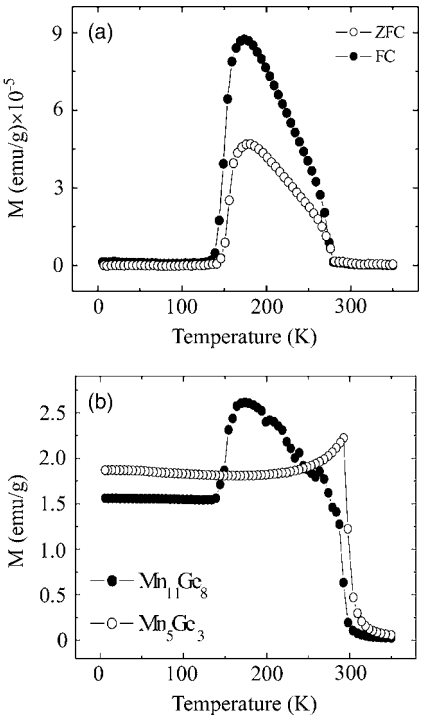

FIG. 3. (a) Temperature-dependent magnetization $M(T)$ of the Mn-poor part of a nominal $Mn_{0.08}Ge_{0.92}$ sample measured in a 10 mT magnetic field under field cooled (solid circle) and zero-field cooled (open circle) conditions. In (b) temperature-dependent magnetization $M(T)$ measured in a 10 mT magnetic field for field cooled $Mn_{11}Ge_8$ (solid circle) and Mn_5Ge_3 (open circles) reference samples is shown.

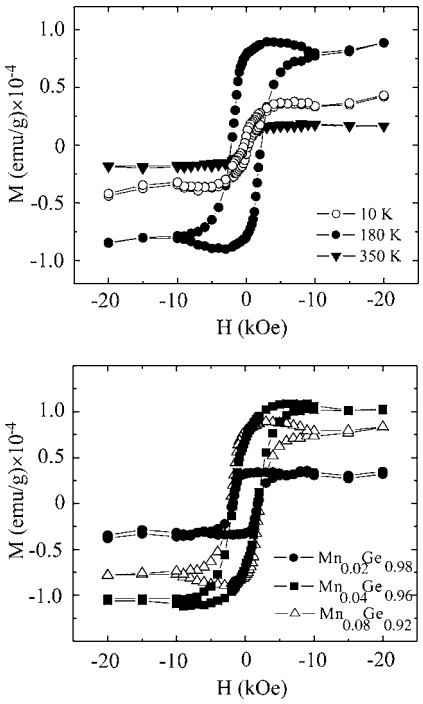

FIG. 4. (a) Magnetic hysteresis loops of the Mn-poor part of the nominal $Mn_{0.08}Ge_{0.92}$ sample recorded at 10 K (open circle), 180 K (solid circle), and 350 K (triangle down). Only at 180 K a distinctive loop is visible due to ferromagnetic behavior. In (b) magnetic hysteresis loops of Mn-poor parts of $Mn_{0.02}Ge_{0.98}$ (solid circle), $Mn_{0.04}Ge_{0.96}$ (solid square), and $Mn_{0.08}Ge_{0.92}$ (open triangle up) samples measured at 180 K are shown.

150 K and an ferromagnetic state to paramagnetic state transition at 285 K. On the other hand, recent investigations on epitaxial Mn_xGe_{1-x} thin films do not show comparable magnetic transitions,[3,4] which was attributed to the absence of Mn-rich alloy phases in the sample.

In order to investigate the origin of this magnetic behavior, we compared the $M(T)$ data obtained from the Mn_xGe_{1-x} samples with the data from two reference samples: $Mn_{11}Ge_8$ and Mn_5Ge_3 [see Fig. 3(b)]. $Mn_{11}Ge_8$ and Mn_5Ge_3 were taken as references, because these compounds can be produced during single-crystal growth.[13] In Fig. 3(b) $M(T)$ curves of both reference compounds (Mn_5Ge_3 and $Mn_{11}Ge_8$) are presented. Mn_5Ge_3 has T_C of about 300 K,[14] whereas for $Mn_{11}Ge_8$ two transition temperatures at 150 and 285 K can be observed, indicating the existence of a ferromagnetic phase between 150 and 285 K. In contrast to the findings by Yamada *et al.*,[15] the magnetization measured below 150 K does not decrease to zero for $Mn_{11}Ge_8$, indicating the presence of a ferromagnetic phase below 150 K. The $Mn_{11}Ge_8$ sample used in the present study possibly contains a small amount of Mn_5Ge_3 responsible for ferromagnetism below 150 K. The Mn-poor part of the nominal $Mn_{0.08}Ge_{0.92}$ sample exhibits two transition temperatures which correlate with the data from the polycrystalline $Mn_{11}Ge_8$ sample. However, no ferromagnetic state was observed in the $Mn_{0.08}Ge_{0.92}$ sample below 150 K. Thus, the ferromagnetic phase found between 150 and 285 K in the $Mn_{0.08}Ge_{0.92}$ is probably due to the $Mn_{11}Ge_8$ phase incorporated into the Ge single crystal. Recent $M(T)$ measurements performed on the MBE-grown Mn_xGe_{1-x} samples also show a transition temperature at about 285 K which is due to the existence of a Mn-rich ordered phase (Mn_5Ge_3) (Ref. 16) and is not an intrinsic property of the DMS. A small divergence of ZFC and FC measurements on the $Mn_{0.08}Ge_{0.92}$ sample is visible which is often attributed to a blocking transition of interacting superparamagnetic Mn-rich clusters of different size incorporated onto Ge matrix as shown by Park *et al.*[17] Recent temperature-dependent magnetization measurements on MBE-grown Mn_xGe_{1-x} samples showed the presence of two different magnetic phases.[18] Superparamagnetic Mn_5Ge_3 clusters were reported to be the origin of a blocking transition at high temperature around 210 K, whereas superparamagnetic Mn-rich nanoclusters cause a blocking transition around 12 K that is attributed to spin-glass behavior.

Figure 4(a) displays magnetic hysteresis loops of the Mn-poor part of the nominal $Mn_{0.08}Ge_{0.92}$ sample measured at different temperatures. Clear ferromagnetic behavior is observed at 180 K. At room temperature the coercive field (H_C) decreases to zero which correlates with the magnetic phase transition at 285 K shown in Fig. 3(a). The saturation magnetization at 180 K is about $5-10\times10^{-5}$ emu/g and the coercive field is about 2 kOe for all Mn_xGe_{1-x} samples [see Fig. 4(b)], showing that different dilution contents have not been achieved during sample preparation, which was also confirmed by EDX measurements. Comparable values of H_C were observed by D'Orazio *et al.*[19] in Mn ion implanted Ge and were attributed to the formation of Mn-rich particles. Moreover, H_C of pure Mn_5Ge_3 (Ref. 20) was found to be in the range of the coercive field measured in our samples.

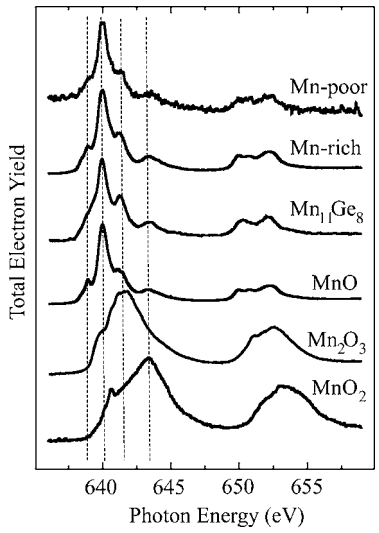

FIG. 5. Mn $L_{2,3}$ XAS spectra of the $Mn_{0.1}Ge_{0.9}$ sample obtained for a Mn-rich and Mn-poor part together with the reference spectra of $Mn_{11}Ge_8$, MnO, Mn_2O_3, and MnO_2.

Thus, ferromagnetic behavior in our samples can be attributed to the Mn-rich particles of a submicron size homogeneously distributed in the Ge matrix.

A linear increase of T_C as a function of increasing Mn dilution content was shown experimentally.[3,6] In the present Mn_xGe_{1-x} samples the transition temperature does not depend on the Mn-content of the samples; in fact, T_C remains constant due to the presence of Mn-rich phase ($Mn_{11}Ge_8$).

C. Electronic properties

In order to investigate the electronic structure of the nominal $Mn_{0.1}Ge_{0.9}$ sample, Mn $L_{2,3}$ XAS measurements were performed for Mn-rich and Mn-poor areas of the $Mn_{0.1}Ge_{0.9}$ sample. Figure 5 shows Mn $L_{2,3}$ XAS spectra obtained from the Mn-rich as well as the Mn-poor regions, together with the reference absorption spectra of $Mn_{11}Ge_8$, MnO (Mn^{2+}), Mn_2O_3 (Mn^{3+}), and MnO_2 (Mn^{4+}). The Mn $L_{2,3}$ XAS spectra of the Mn-rich and Mn-poor parts of the $Mn_{0.1}Ge_{0.9}$ sample show similar line shapes which are close to that of MnO but quite different from Mn_2O_3 and MnO_2, suggesting that most of the Mn is present in the Mn^{2+} state. Thus, the existence of metallic Mn in the Mn-rich as well as in the Mn-poor parts of the $Mn_{0.1}Ge_{0.9}$ sample can be ruled out. The XAS spectra of the Mn-poor part showed a lower intensity compared with that of the Mn-rich part, confirming a lower Mn concentration (the XAS spectra in Fig. 5 were normalized to the maximum intensity). A comparable Mn $L_{2,3}$ XAS line shape was reported by Kang *et al.*[12] measured on the inhomogeneous DMS Mn_xGe_{1-x}. The spectra are also found to be in good agreement with the XAS spectrum calculated for the tetrahedrally coordinated Mn^{2+} in the high-spin ($S=5/2$) configuration.[12]

Figure 6 shows valence band photoelectron spectroscopy of the Mn-poor part of the $Mn_{0.1}Ge_{0.9}$ sample performed around the Mn $2p_{3/2}$ absorption edge. The off-resonance spectrum ($h\nu=634$ eV) shows a line shape similar to that of pure Ge which is expected from the small Mn concentration. The spectral line shape of the on-resonance spectra ($h\nu=640$ eV) measured for the Mn-poor part of the Mn_xGe_{1-x} samples shows a broad feature around 4.8 eV, which is in agreement with previous studies on phase-separated Mn_xGe_{1-x}.[12,21] The difference between the on-resonance and off-resonance spectra is proportional to the Mn 3*d* PDOS. The extracted Mn 3*d* PDOS exhibits a peak centered at 4.8 eV and a weak tail up to 11 eV. The Mn 3*d* PDOS shows that Mn 3*d* states are located well below E_F, indicating that Mn 3*d* electrons occupy the deep levels. The peak in Mn 3*d* PDOS centered at 4.8 eV is in good agreement with a similar feature of the Mn_5Ge_3 phase[21] as well as of the ion implanted Mn_xGe_{1-x} samples containing Mn_5Ge_3 nanoparticles.[22] Moreover, the spectral features related to the effective dilution of substitutional Mn in the Ge are expected to appear at about 4 eV,[22] which is not in agreement with our measurements. Thus, the present PES measurements give a strong indication that even in the Mn-poor part of the Mn_xGe_{1-x} sample Mn is present in the form of Mn-rich phase Mn_5Ge_3.

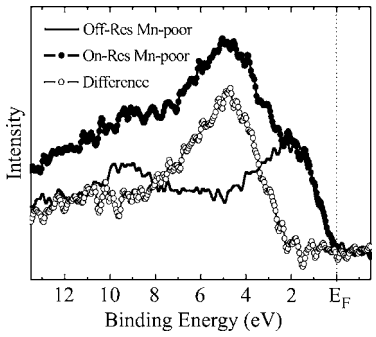

FIG. 6. Resonant photoemission spectroscopy of the Mn-poor part of the $Mn_{0.1}Ge_{0.9}$ sample around the Mn $2p_{3/2}$ absorption edge. On-resonance ($h\nu=640$ eV) and off-resonance ($h\nu=634$ eV) valence band spectra together with the difference curve (open circle) reflecting the Mn 3*d* PDOS are shown.

IV. CONCLUSION

In conclusion, we investigated structural, magnetic, and electronic properties of Mn_xGe_{1-x} samples grown by the Bridgman's crystal growth technique. EDX used for the investigation of the chemical distribution of Mn in Ge clearly shows a strong phase separation into the single-crystalline homogeneous Mn-poor phase containing 1%–3% of Mn and the highly inhomogeneous Mn-rich phase containing the regions having the composition close to Mn_5Ge_3 and $Mn_{11}Ge_8$ phases. Temperature-dependent magnetization measurements on the Mn-poor part of the Mn_xGe_{1-x} samples show ferromagnetic transitions at 150 and 285 K which correspond to those of the $Mn_{11}Ge_8$ reference sample. The observed magnetic behavior in both parts of the sample can be attributed to the Mn-rich submicron-sized clusters homogeneously distributed in the Ge matrix. Mn $L_{2,3}$ XAS measurements show that Mn ions in the Mn-rich and Mn-poor parts are present in the divalent high-spin state. The presence of the Mn-rich phases in the Mn-poor parts was also demonstrated with ResPES measurements performed at the Mn $2p_{3/2}$ absorption edge. The obtained Mn 3*d* PDOS shows a feature centered at 4.8 eV which is characteristic for the Mn_5Ge_3 phase. In this study we demonstrate that ferromagnetism observed in both

parts of the Mn_xGe_{1-x} samples is due to the Mn-rich clusters in the strongly phase-separated Mn_xGe_{1-x}, indicating that the single-crystal growth technique is not an appropriate method for the DMS preparation.

ACKNOWLEDGMENTS

We would like to thank U. Probst for fruitful discussions. E.B. and M.F. acknowledge the financial support by BESSY (Berlin). Part of this work was supported by SFB 513.

[1]H. Ohno, Science **281**, 951 (1998).
[2]T. Dietl, H. Ohno, F. Matsukura, J. Cibert, and D. Ferrand, Science **287**, 1019 (2000).
[3]Y. D. Park, A. T. Hanbicki, S. C. Erwin, C. S. Hellberg, J. M. Sullivan, J. E. Mattson, T. F. Ambrose, A. Wilson, G. Spanos, and B. T. Jonker, Science **295**, 651 (2002).
[4]F. D'Orazio, F. Lucari, N. Pinto, L. Morresi, and R. Murri, J. Magn. Magn. Mater. **272–276**, 2006 (2004).
[5]S. Cho, S. Choi, S. C. Hong, Y. Kim, J. B. Ketterson, B.-J. Kim, Y. C. Kim, and J.-H. Jung, Phys. Rev. B **66**, 033303 (2002).
[6]F. Tsui, L. He, L. Ma, A. Tkachuk, Y. S. Chu, K. Nakajima, and T. Chikyow, Phys. Rev. Lett. **91**, 177203 (2003).
[7]A. P. Li, J. F. Wendelken, J. Shen, L. C. Feldman, J. R. Thompson, and H. H. Weitering, Phys. Rev. B **72**, 195205 (2005).
[8]D. Bougeard, S. Ahlers, A. Trampert, N. Sircar, and G. Abstreiter, Phys. Rev. Lett. **97**, 237202 (2006).
[9]S. Ahlers, D. Bougeard, N. Sircar, G. Abstreiter, A. Trampert, M. Opel, and R. Gross, Phys. Rev. B **74**, 214411 (2006).
[10]L. Lifeng, C. Nuofu, C. Chenlong, L. Yanli, Y. Zhigang, and Y. Fei, J. Cryst. Growth **273**, 106 (2004).
[11]S. Picozzi, L. Ottaviano, M. Passacantando, G. Profeta, A. Continenza, F. Priolo, M. Kim, and A. J. Freeman, Appl. Phys. Lett. **86**, 062501 (2005).
[12]J.-S. Kang, G. Kim, S. C. Wi, S. S. Lee, S. Choi, S. Cho, S. W. Han, K. H. Kim, H. J. Song, H. J. Shin, A. Sekiyama, S. Kasai, S. Suga, and B. I. Min, Phys. Rev. Lett. **94**, 147202 (2005).
[13]*Binary Alloy Phase Diagrams*, 2nd ed., edited by T. B. Massalski (ASM International, Materials Park, OH, 1990).
[14]X. B. Liu and Z. Altounian, J. Appl. Phys., **99**, 08Q101 (2006).
[15]N. Yamada, K. Maeda, Y. Usami, and T. Ohoyama, J. Phys. Soc. Jpn. **55**, 3721 (1986).
[16]C. Bihler, C. Jaeger, T. Vallaitis, M. Gjukic, M. S. Brandt, E. Pippel, J. Woltersdorf, and U. Gösele, Appl. Phys. Lett. **88**, 112506 (2006).
[17]Y. D. Park, A. Wilson, A. T. Hanbicki, J. E. Mattson, T. Ambrose, G. Spanos, and B. T. Jonker, Appl. Phys. Lett. **78**, 2739 (2001).
[18]C. Jaeger, C. Bihler, T. Vallaitis, S. T. B. Goennenwein, M. Opel, R. Gross, and M. S. Brandt, Phys. Rev. B **74**, 045330 (2006).
[19]F. D'Orazio, F. Lucari, M. Passacantando, P. Picozzi, S. Santucci, and A. Verna, IEEE Trans. Magn. **38**, 2856 (2002).
[20]C. Zeng, S. C. Erwin, L. C. Feldman, A. P. Li, R. Jin, Y. Song, J. R. Thompson, and H. H. Weitering, Appl. Phys. Lett. **83**, 5002 (2003).
[21]C. Zeng, W. Zhu, S. C. Erwin, Z. Zhang, and H. H. Weitering, Phys. Rev. B **70**, 205340 (2004).
[22]L. Ottaviano, M. Passacantando, S. Picozzi, A. Continenza, R. Gunnella, A. Verna, G. Bihlmayer, G. Impellizzeri, and F. Priolo, Appl. Phys. Lett. **88**, 061907 (2006).